

## Observational constraints on power law Starobinsky inflation

Saisandri Saini and Akhilesh Nautiyal

*Department of Physics, Malaviya National Institute of Technology,  
Jaipur, JLN Marg, Jaipur-302017, India*

 (Received 30 May 2023; accepted 14 November 2023; published 1 December 2023)

In this work we revisit power law,  $\frac{1}{M^2}R^\beta$ , inflation to find the deviations from  $R^2$  inflation allowed by current cosmic microwave background (CMB) and large-scale structure (LSS) observations. We compute the power spectra for scalar and tensor perturbations numerically and perform Markov chain Monte Carlo analysis to put constraints on parameters  $M$  and  $\beta$  from Planck-2018, BICEP3 and other LSS observations. We consider general reheating scenario and also vary the number of  $e$ -foldings during inflation,  $N_{\text{pivot}}$ , along with the other parameters. We find  $\beta = 1.966_{-0.042}^{+0.035}$ ,  $M = (3.31_{-2}^{+5}) \times 10^{-5}$  and  $N_{\text{pivot}} = 41_{-10}^{+10}$  with 95% C.L. This indicates that the current observations allow deviation from Starobinsky inflation. The scalar spectral index,  $n_s$ , and tensor-to-scalar ratio,  $r$ , derived from these parameters, are consistent with the Planck and BICEP3 observations.

DOI: [10.1103/PhysRevD.108.123505](https://doi.org/10.1103/PhysRevD.108.123505)

### I. INTRODUCTION

The idea of inflation [1] was introduced to solve various problems of the big bang theory. Later it was realized [2–4] that it provides seeds for cosmic microwave background (CMB) anisotropy and large-scale structure (LSS) of the Universe. During inflation the potential energy of a scalar field, named as inflaton, dominates the energy density of the universe for a very short period of time. The quantum fluctuations in the inflaton field, which are coupled to the metric fluctuations, generate primordial density perturbations. There are also quantum fluctuations in the spacetime geometry during inflation responsible for the primordial gravitational waves, also known as tensor perturbations. Inflation predicts nearly scale invariant, adiabatic and Gaussian perturbations that are in excellent agreement with various CMB observations such as COBE [5], WMAP [6], and Planck [7,8]. The choices for inflaton potential are derived from various particle physics models and string theory, which provide a large class of inflaton potentials [9]; however, we lack a unique model of inflation.

The first self-consistent model of inflation was proposed by Starobinsky in 1980 [10], where inflation is achieved by  $\frac{1}{M^2}R^2$  interaction,  $R$  being the Ricci scalar, in the Einstein-Hilbert action without additional scalar field. Transforming to the Einstein frame, the  $R^2$  Starobinsky model gives rise to plateau potential of the inflaton field. The  $R^2$  Starobinsky inflation is of great interest as it is one of the best-suited models of inflation from recent Planck observations [8], and it also incorporates a graceful exit to the radiation dominated epoch via a period of reheating [11–13], where

the standard model particles are created through the oscillatory decay of the inflaton, called a scalaron in the case of  $R^2$  inflation.

In this work, we investigate the generalization of Starobinsky inflation by considering a power law,  $\frac{1}{6M^2} \frac{R^\beta}{M_{\text{pl}}^{2\beta-2}}$ , correction to the Einstein-Hilbert action. Here  $\beta \approx 2$  and not necessarily an integer, allowing a small deviation from  $\beta = 2$ . The  $R^\beta$  Lagrangian was first considered in the context of higher-order metric theories of gravity [14,15] and was then applied to inflation [16,17] as a generalization of  $R^2$  inflation (see also [9,18–20] for a detailed review). It was shown in [21–23] that  $R^\beta$  term, with  $\beta$  slightly different from 2 can arise as a quantum correction to the Starobinsky  $R^2$  term in the Einstein-Hilbert action. It was also shown in [24] that the models of Higgs field as inflaton with local Weyl symmetry are equivalent to generalized Starobinsky inflation in Einstein frame. Power law terms in the Einstein-Hilbert action in the Jordan frame can be reconstructed from various scalar potentials in Einstein frame [25]. It has also been shown in [26] that the power-law Starobinsky inflation can be embedded into a general class T-models [27]. Modifications to  $R^2$ -term has also been obtained in [28] by considering quasi-de Sitter evolution in  $f(R)$  gravity.  $R^\beta$  inflation became popular in 2014 when BICEP2 reported large value of tensor-to-scalar ratio [29]  $r = 0.2_{-0.05}^{+0.07}$ . It was shown [21,24,30] that this model could generate large  $r$  compared to  $R^2$  inflation for  $\beta$  slightly smaller than 2. However, it was found later that the BICEP2 signal of  $B$ -mode polarization is not of primordial origin, but due to an unknown amplitude of foreground dust emission [31]. The  $R^\beta$  Lagrangian was also

used to construct a unified model of inflation and dark energy in  $f(R)$  gravity [32]. It is shown in [33,34] that the presence of the Chern-Simons term along with  $R^\beta$  can significantly reduce the tensor-to-scalar ratio as well as predicting axions as dark matter candidates.

Another interesting aspect of Starobinsky inflation is that a no-scale supergravity model of inflation with a modulus field and the inflaton field with a minimal Wess-Zumino superpotential gives the same  $F$ -term potential in the Einstein frame as the Starobinsky model [35]. It was shown in [36,37] that there are various possible scenarios of no-scale supergravity that can reproduce the effective potential of the Starobinsky model and other related models. The Starobinsky model can also be derived from the  $D$ -term potential in supergravity models of inflation [38–41]. A no-scale supergravity model, with inflaton potential equivalent to power law Starobinsky potential in Einstein frame, was obtained in [42] by using a  $(\Phi + \bar{\Phi})^n$  term in the no-scale Kähler potential with the Wess-Zumino form of the superpotential.

It was also shown in [42] that a small deviation from  $\beta = 2$  can give the tensor-to-scalar ratio  $r \sim O(0.1)$ . The analysis of [42] was limited to  $\beta \leq 2$  and they used slow-roll approximation to obtain the observational constraint on the model parameters. The consistency relations among the scalar spectral index, the tensor-to-scalar ratio and the running of scalar spectral index were derived in [43] and the observational constraints on  $\beta$  were found for various choices of  $n_s$ ,  $r$ , and  $N_k$ , again using the slow-roll approximation. However, the parameter  $\beta$  (denoted by  $p$  in [43]) was varied between 1.80 and 2.1 for the analysis. The attractor solutions for the  $R^\beta$  model in the Jordan and the Einstein frame, for  $1.9 \leq \beta \leq 2.01$ , were also studied in [44], and it was shown, using slow-roll conditions, that  $R^\beta$  inflation is viable in both the frames. Observational constraints on  $R^\beta$  inflation are also obtained in [45] numerically integrating the perturbation equations, however, the entire region of the parameter space is not explored and only some selected values of  $\beta$  are used. The variations from the Starobinsky potential in the Einstein frame has also been studied in [46] based on a potential derived from brane inflation, and it is found that the data allows a deviation from the Starobinsky model.

In our work we use MODECODE [47] to explore the parameter space of  $R^\beta$  model. In MODECODE the background and perturbation equations for inflation are solved numerically without the usual slow-roll approximation, and the power spectra for scalar and tensor perturbations are computed. These power spectra are used in CAMB [48] to compute the angular power spectra for CMB anisotropy and polarization, which is then interfaced with COSMOMC [49], which performs the Markov chain Monte Carlo (MCMC) analysis for parameter estimation. With MODECODE the parameters of inflationary potential can

be constrained directly from the CMB observations; the standard inflationary parameters, like  $r$ ,  $n_s$  are treated as derived parameters. We vary  $\beta$  between 1.9 to 2.07 along with  $M$  and  $N_{\text{pivot}}$  to find the best-fit parameters of the model and to look for any deviation from Starobinsky model,  $\beta = 2$ .

The paper is organized as follows. In Sec. II we obtain the potential for the power law Starobinsky model in Einstein frame using conformal transformations. In Sec. III we obtain the equation of motion for scalar field and perturbation equations used in MODECODE. In Sec. IV we compute the CMB power spectra using MODECODE and CAMB and use COSMOMC to put constraints on the parameters of power law Starobinsky inflation. We summarize our results and give our conclusions in Sec. V.

## II. POWER LAW STAROBINSKY MODEL

The power law Starobinsky inflation is a special case of  $f(R)$  gravity, where the action is given as [18,19]

$$S_J = \frac{-M_{\text{Pl}}^2}{2} \int \sqrt{-g} f(R) d^4x. \quad (1)$$

For power law Starobinsky inflation the function  $f(R)$  has the form [42]

$$f(R) = \left( R + \frac{1}{6M^2} \frac{R^\beta}{M_{\text{Pl}}^{2\beta-2}} \right), \quad (2)$$

where  $M_{\text{Pl}}^2 = (8\pi G)^{-1}$ ,  $g$  is the determinant of the metric  $g_{\mu\nu}$ , and  $M$  is a dimensionless real parameter. The subscript  $J$  in Eq. (1) stands for Jordan frame, where the action is a nonlinear function of the Ricci scalar. We can rewrite Eq. (1) as

$$S_J = \int d^4x \sqrt{-g} \left( \frac{-M_{\text{Pl}}^2}{2} FR + U \right), \quad (3)$$

where

$$U = \frac{(FR - f)M_{\text{Pl}}^2}{2}. \quad (4)$$

Here,  $F$  is the first derivative of  $f(R)$  with respect to  $R$ . The action in the Einstein frame can be obtained with the conformal transformation  $\tilde{g}_{\mu\nu}(x) = \Omega(x)g_{\mu\nu}(x)$ , where  $\Omega$  is the conformal factor and a tilde represents quantities in the Einstein frame.

The Ricci scalar  $R$  in the Jordan frame is related to the Ricci scalar  $\tilde{R}$  in the Einstein frame as

$$R = \Omega \left( \tilde{R} + 3\tilde{\square}\omega - \frac{3}{2}\tilde{g}^{\mu\nu}\partial_\mu\omega\partial_\nu\omega \right), \quad (5)$$

where  $\omega \equiv \ln \Omega$ ,  $\tilde{\square}\omega \equiv \frac{1}{\sqrt{-\tilde{g}}}\partial_\mu(\sqrt{-\tilde{g}}\tilde{g}^{\mu\nu}\partial_\nu\omega)$  and  $\partial_\mu\omega = \frac{\partial\omega}{\partial\tilde{x}^\mu}$ . We choose  $\Omega = F$  to obtain the action in the Einstein frame and also introduce a new scalar field  $\chi$  defined by

$$\chi \equiv \sqrt{\frac{3}{2}}M_{\text{Pl}} \ln F. \quad (6)$$

This gives  $\Omega = \exp(\frac{2\chi}{\sqrt{6}M_{\text{Pl}}})$ . The action Eq. (1) gets transformed to an Einstein-Hilbert form using Eq. (5) and relation  $\sqrt{-g} = \Omega^{-2}\sqrt{-\tilde{g}}$  as

$$S_E = \int d^4x \sqrt{-\tilde{g}} \left( \frac{-M_{\text{Pl}}^2}{2} \tilde{R} + \frac{1}{2} \tilde{g}^{\mu\nu} \partial_\mu \chi \partial_\nu \chi + V(\chi) \right), \quad (7)$$

where  $V(\chi)$  is the Einstein-frame potential given by

$$V(\chi) = \frac{(RF(R) - f(R))M_{\text{Pl}}^2}{2F(R)^2}. \quad (8)$$

The potential (8) for power law Starobinsky model (2) in the Einstein frame becomes

$$V(\chi) = \left( \frac{\beta-1}{2} \right) \left( \frac{6M^2}{\beta^\beta} \right)^{\frac{1}{\beta-1}} \exp \left[ \frac{2\chi}{\sqrt{6}} \left( \frac{2-\beta}{\beta-1} \right) \right] \times \left( 1 - \exp \left( \frac{-2\chi}{\sqrt{6}} \right) \right)^{\frac{\beta}{\beta-1}}, \quad (9)$$

where we have taken  $M_{\text{Pl}} = 1$  and we will use this from now on. We can also see that, for  $\beta = 2$ , the potential (9) reduces to Starobinsky  $R^2$  inflation. The potential (9) for various choices of  $\beta$  around  $\beta = 2$  is depicted in Fig. 1. The slow-roll inflation occurs in the regime where  $\chi > 0$ . The potential is flat for  $\beta = 2$  for large values of  $\chi$  and it asymptotically approaches a constant value. However, the potential gets steeper for  $\beta < 2$ , which gives larger tensor-to-scalar ratio as compared to  $\beta = 2$ . In case of  $\beta > 2$  the

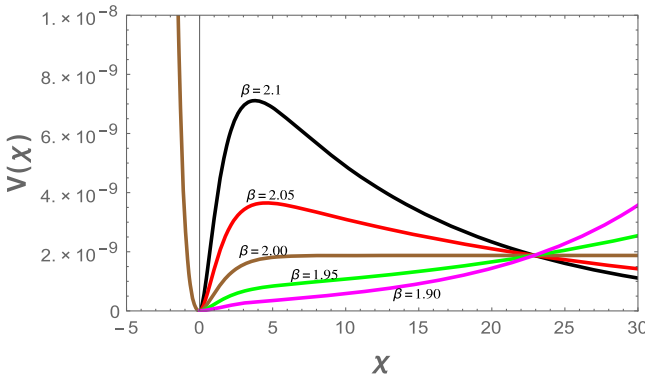


FIG. 1. The potential (9) for various values of  $\beta$ . The value of  $M$  is fixed at  $M = 5 \times 10^{-5}$ , and the values of potential and scalar field are in  $M_p = 1$  units.

potential first increases with  $\chi$  and attains a maximum value at  $\chi = M_{\text{Pl}} \sqrt{\frac{3}{2}} \ln \left[ \frac{2(\beta-1)}{\beta-2} \right] \equiv \chi_m$ , then it decreases and goes to zero for large  $\chi$ . Thus, the inflation can occur for  $\chi$  rolling between  $0 \leq \chi \leq \chi_m$  or  $\chi > \chi_m$ . We will consider  $\chi < \chi_m$  for our analysis to study the deviation from  $R^2$  inflation. We solve the background evolution equations and perturbation equations using potential (9) numerically using MODECODE. The necessary equations are discussed in the proceeding section.

### III. INFLATIONARY DYNAMICS

#### A. Background equations

We analyze the power law Starobinsky inflation in the Einstein frame. During inflation the energy density of the scalar field  $\chi$  dominates the Universe, and hence the expansion is governed by the Friedmann equations,

$$H^2 = \frac{1}{3M_{\text{Pl}}^2} \left[ \frac{1}{2} \dot{\chi}^2 + V(\chi) \right], \quad (10)$$

$$\dot{H} = -\frac{1}{2M_{\text{Pl}}^2} \dot{\chi}^2. \quad (11)$$

The equation of motion for  $\chi$  is the Klein-Gordon equation in an expanding spacetime,

$$\ddot{\chi} + 3H\dot{\chi} + \frac{dV(\chi)}{d\chi} = 0. \quad (12)$$

Here, the dot stands for the differentiation with respect to cosmic time. Since we choose the number of  $e$ -folding,  $N = \ln a$  as the independent variable to solve mode equations numerically, the background equations for Hubble parameter Eqs. (10) and (11) and the scalar field  $\chi$  Eq. (12) are expressed in terms of  $N$  as

$$H^2 = \frac{\frac{1}{3M_{\text{Pl}}^2} V(\chi)}{1 - \frac{1}{6M_{\text{Pl}}^2} \dot{\chi}^2}, \quad (13)$$

$$H' = -\frac{1}{2M_{\text{Pl}}^2} H \dot{\chi}^2, \quad (14)$$

and

$$\chi'' + \left( \frac{H'}{H} + 3 \right) \chi' + \frac{1}{H^2} \frac{dV(\chi)}{d\chi} = 0, \quad (15)$$

where prime denotes the differentiation with respect to  $N$ . These background equations are solved numerically by setting the initial conditions such that the field velocity is at its slow-roll value. This makes sure that the (small) initial transient in the velocity is damped away. The solution is then used as an input to perturbations equations.

### B. Perturbation equation

The density perturbations generated during inflation are described by gauge-invariant comoving curvature perturbations  $\mathcal{R}$ , which is related to Mukhanov-Sasaki variable  $u$  as [50,51]

$$u = -z\mathcal{R}, \quad (16)$$

where  $z = \frac{1}{H} \frac{dz}{d\tau}$ ,  $\tau$  denotes the conformal time. The quantity  $z$  depends on the background evolution and can be determined by solving Eqs. (14) and (15). The evolution equation for Fourier mode  $u_k$  in conformal time is given as

$$\frac{d^2 u_k}{d\tau^2} + \left( k^2 - \frac{1}{z} \frac{d^2 z}{d\tau^2} \right) u_k = 0. \quad (17)$$

The primordial power spectrum is defined in terms of the two-point correlation function of comoving curvature perturbation as

$$\mathcal{P}_{\mathcal{R}} = \frac{k^3}{2\pi^2} \langle \mathcal{R}_k \mathcal{R}_{k'}^* \rangle \delta^3(k - k'), \quad (18)$$

which is related to Mukhanov-Sasaki variable  $u_k$  (16) as

$$\mathcal{P}_{\mathcal{R}}(k) = \frac{k^3}{2\pi^2} \left| \frac{u_k}{z} \right|^2, \quad (19)$$

Similarly the mode equation for tensor perturbations generated during inflation is given as

$$\frac{d^2 v_k}{d\tau^2} + \left( k^2 - \frac{1}{a} \frac{d^2 a}{d\tau^2} \right) v_k = 0, \quad (20)$$

and the primordial tensor power spectrum is given as

$$\mathcal{P}_t(k) = \frac{4}{\pi^2} \frac{k^3}{M_{\text{Pl}}^2} \left| \frac{v_k}{a} \right|^2. \quad (21)$$

To obtain the scalar and tensor power spectra, the mode equations (17) and (20) are solved numerically. As we choose  $e$ -foldings  $N = \ln a$  as independent variables to solve these equations, the background quantity  $z = \chi'$ . Hence Eqs. (17) and (20) can be written in terms of  $N$  as

$$u_k'' + \left( \frac{H'}{H} + 1 \right) u_k' + \left\{ \frac{k^2}{a^2 H^2} - \left[ 2 - 4 \frac{H'}{H} \frac{\chi''}{\chi'} - 2 \left( \frac{H'}{H} \right)^2 - 5 \frac{H'}{H} - \frac{1}{H^2} \frac{d^2 V}{d\chi^2} \right] \right\} u_k = 0, \quad (22)$$

$$v_k'' + \left( \frac{H'}{H} + 1 \right) v_k' + \left[ \frac{k^2}{a^2 H^2} - \left( \frac{H'}{H} + 2 \right) \right] v_k = 0. \quad (23)$$

The numerical solutions of Eqs. (22) and (23) are obtained along with the background equations (14), (15) using Bunch-Davies initial conditions.

The scalar spectral index  $n_s$  and the tensor spectral index  $n_t$  are determined from the power spectra obtained numerically using their definitions [52]

$$n_s = 1 + \frac{d \ln \mathcal{P}_{\mathcal{R}}}{d \ln k}, \quad (24)$$

$$n_t = \frac{d \ln \mathcal{P}_t}{d \ln k}. \quad (25)$$

The tensor-to-scalar ratio  $r$  is defined by [52]

$$r = \frac{\mathcal{P}_t}{\mathcal{P}_{\mathcal{R}}}. \quad (26)$$

Planck CMB observations provide constraints on  $n_s$  and  $r$ . However, in our analysis they are derived parameters, and the parameters of the inflaton potential (9),  $M$  and  $\beta$ , are directly constrained from the CMB observations.

### IV. OBSERVATIONAL CONSTRAINTS

To calculate the scalar and tensor power spectrum for the quantum fluctuations generated during inflation, we modify the publicly available MODECODE [47] for the power law Starobinsky potential (9) in the Einstein frame. We consider the general reheating scenario, where the parameter  $N_{\text{pivot}}$  that represents the number of  $e$ -foldings from the end of inflation to the time when length scales correspond the Fourier mode  $k_{\text{pivot}}$  leave the Hubble radius during inflation, is also varied along with other potential parameters. MODECODE can be used within CAMB [48]. To compute the primordial power spectra at arbitrary values of  $k$  in CAMB, MODECODE uses cubic spline interpolation on a grid of  $k$  values spaced evenly in  $\ln k$ . CAMB computes the angular power spectra for CMB anisotropy and polarization. These CMB power spectra are used in COSMOMC to put constraints on the parameters of the inflaton potential along with the other parameters of the cold dark matter ( $\Lambda$ CDM) model from various CMB and large-scale structure observations. To constrain the parameters  $M$  and  $\beta$  of inflaton potential (9) we use Planck-2018 data along with BICEP3 [53], baryon acoustic oscillation (BAO) and Pantheon data. The priors for the parameters of inflaton potential and  $N_{\text{pivot}}$  are given in Table I. The priors for the parameter  $M$  are sampled logarithmically to cover a large range. The parameter  $\beta$  is varied around 2 to consider deviation from Starobinsky inflation. The other parameters of the  $\Lambda$ CDM model are also varied along with these three parameters with priors given in [54]. For each parameter the MCMC convergence diagnostic tests is performed over the four chains using the Gelman and Rubin variance of mean/mean of chain variance  $R - 1$  statistics.

TABLE I. Priors on model parameters.

$\log_{10}M$	$-6.5 < \log_{10}M < -3.0$
$\beta$	$1.90 < \beta < 2.07$
$N_{\text{pivot}}$	$25 < N_{\text{pivot}} < 90$

TABLE II. Planck-2018, BICEP3 and BAO constraints on parameters of potential,  $r$  and  $n_s$ .

Parameter	68% limits	95% limits	99% limits
$\log_{10}M$	$-4.48^{+0.23}_{-0.26}$	$-4.48^{+0.40}_{-0.40}$	$-4.48^{+0.50}_{-0.45}$
$\beta$	$1.966^{+0.027}_{-0.015}$	$1.966^{+0.035}_{-0.042}$	$1.966^{+0.039}_{-0.056}$
$N_{\text{pivot}}$	$41^{+6}_{-10}$	$41^{+10}_{-10}$	$41^{+20}_{-10}$
$n_s$	$0.9688 \pm 0.0036$	$0.9688^{+0.0072}_{-0.0071}$	$0.9688^{+0.0094}_{-0.0094}$
$r$	$0.0198^{+0.0043}_{-0.016}$	$0.020^{+0.030}_{-0.017}$	$0.020^{+0.048}_{-0.018}$

The constraints obtained for parameters of potential (9), the  $e$ -foldings  $N_{\text{pivot}}$  and the deriver parameters,  $r$  and  $n_s$ , are shown in Table II.

It is evident from the Table that the best fit value of  $\beta$  is

$$\beta = 1.966^{+0.035}_{-0.042}, \quad 95\% \text{ C.L.}, \quad (27)$$

which indicates that the Planck observations favor deviation from Starobinsky model,  $\beta = 2$ , which lies within  $2\sigma$  of the best-fit value (27). The power law Starobinsky model prefers the number of  $e$ -foldings,

$$N_{\text{pivot}} = 41^{+10}_{-10}, \quad 95\% \text{ C.L.}, \quad (28)$$

It can also be seen from the Table II that the best-fit values of scalar spectral index  $n_s$  and tensor-to-scalar ratio  $r$  derived from the best-fit values of potential parameters, for the power law Starobinsky model, is well within the Planck bounds. The marginalized probability distributions for various inflationary parameters are shown in Fig. 2.

The joint 68% C.L. and 95% C.L. constraints on the potential parameters  $\beta$  and  $M$ , and  $N_{\text{pivot}}$  are shown in Figs. 3 and 4.  $\beta$  and  $M$  from Planck-2018 and BICEP3 [53] data are presented in Fig. 3(a), which shows that the two parameters are strongly correlated. The potential parameter  $\beta$  is also strongly correlated with the number of  $e$ -foldings  $N_{\text{pivot}}$ , as can be seen from the joint constraints on  $\beta$  and  $N_{\text{pivot}}$  in Fig. 3(b). It is evident from the figure that more the deviation from the Starobinsky model, the lesser  $e$ -foldings are preferred by the Planck-2018 observations. Figure 4 indicates that  $N_{\text{pivot}}$  is also strongly correlated with the potential parameter  $M$ .

The joint constraints on  $r$  and  $n_s$  are shown in Fig. 5. Here these two parameters are derived parameters and the

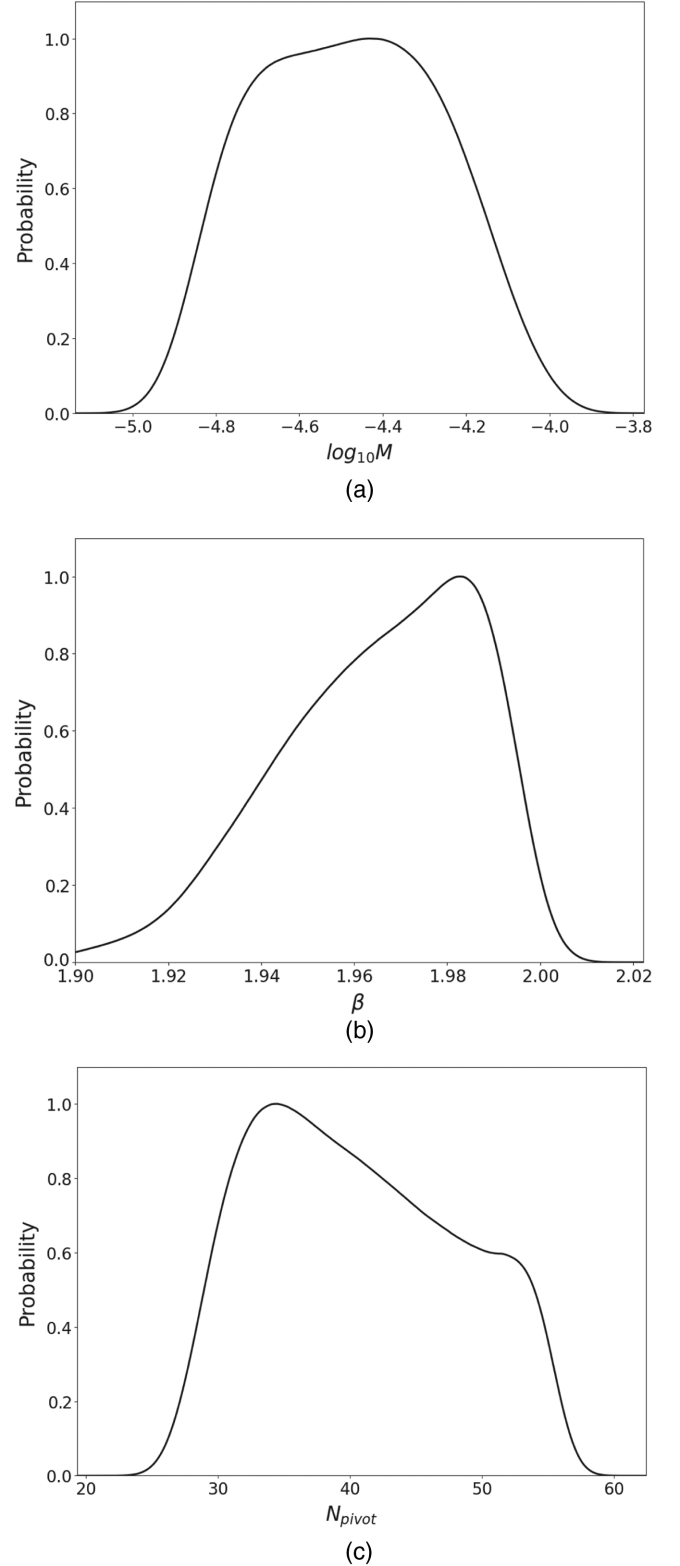


FIG. 2. Marginalized constraints on the potential parameters and  $N_{\text{pivot}}$  using Planck-2018, BICEP3 and BAO data.

constraints on these two parameters are derived from the constraints on the potential parameters and  $N_{\text{pivot}}$ , which are used as an input parameters for MCMC analysis.

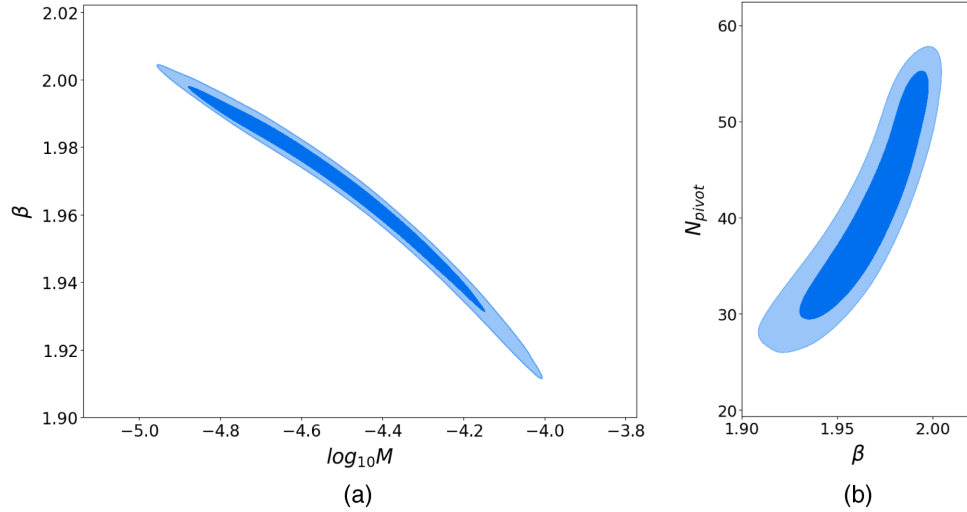


FIG. 3. Joint 68% C.L., and 95% C.L. constraints on parameters of potential and  $N_{\text{pivot}}$  using Planck-2018, BICEP3, and BAO data.

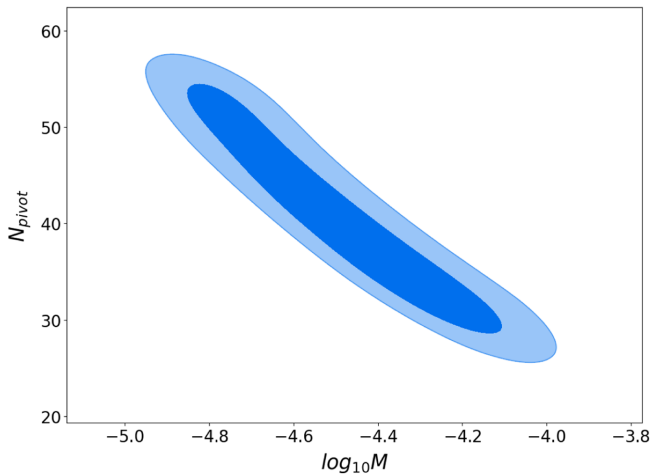


FIG. 4. Joint 68% C.L., and 95% C.L. constraints on potential parameter  $M$  and  $N_{\text{pivot}}$  from Planck-2018, BICEP3, and BAO data.

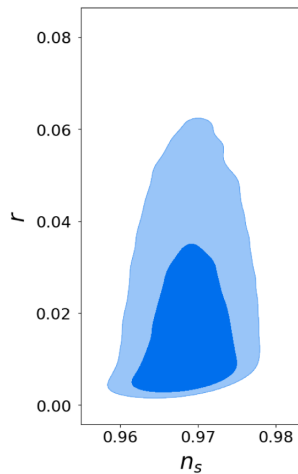


FIG. 5. Joint 68% C.L., and 95% C.L. constraints on  $n_s$  and  $r$  from Planck-2018, BICEP3, and BAO data.

## V. CONCLUSIONS

The  $R^\beta$  term in Einstein Hilbert action with  $\beta$  slightly different from 2 arises as a quantum correction to the Starobinsky  $R^2$  term [21–23]. Inflation with  $R^\beta$  term, named the power law Starobinsky inflation, was first considered in [16,17]. This model gained popularity in 2014 after BICEP2 reported large tensor-to-scalar ratio, and it was shown by [21,24,30] that large  $r$  can be generated in  $R^\beta$  inflation with  $\beta$  slightly less than 2. The analysis of power law Starobinsky inflation was further done by [42–44] using slow-roll approximation, and constraints on the parameters of the potential (9),  $\beta$  and  $M$ , were obtained from CMB constraints on inflationary parameters  $n_s$  and  $r$ .

In this work we analyze power law Starobinsky inflation, in the light of Planck-2018 and BICEP3 [53] CMB observations and other large-scale structure observations. We use the inflaton potential (9) for power law Starobinsky inflation in the Einstein frame. We evaluate the power spectra for scalar and tensor perturbations numerically using MODECODE. With the help of this we perform MCMC analysis using COSMOC to put constraints on the inflaton potential parameters  $\beta$  and  $M$ , and the number of  $e$ -foldings  $N_{\text{pivot}}$ . We vary  $\beta$  between 1.9 to 2.07 to consider deviation from the Starobinsky inflation. We find from Planck-2018 and BICEP3 [53] observations that  $\beta = 1.966^{+0.035}_{-0.042}$ , 95% C.L. This implies that the current CMB and LSS observations prefer slight deviation from Starobinsky inflation. The value  $\beta = 2$  lies within  $2\sigma$  of the best fit value. For our analysis we consider the general reheating scenario and we find that the number of  $e$ -foldings from the end of inflation to the time when pivot scale  $k_{\text{pivot}}$  leaves the inflationary horizon  $N_{\text{pivot}} = 41 \pm 10$ , 95% C.L. We also find that the number of  $e$ -foldings and the parameters  $M$  and  $\beta$  are strongly correlated Figs. 3 and 4. Planck-2018 data prefers

smaller  $N_{\text{pivot}}$  for larger deviation from the Starobinsky inflation.

Deviation from  $\beta = 2$  was also found in the analysis done by [43–45] using slow-roll approximation. In [43] selective values of  $n_s$  and  $r$ , allowed by Planck-2013 data, were used to find values of  $\beta$  (denoted by  $p$  there) and  $N_{\text{pivot}}$ , and it was shown that  $1.9 \leq \beta \leq 2$ . It is also found in [43] that  $(\beta, N_{\text{pivot}}) = (1.93, 30)$  for  $(n_s, r) = (0.96, 0.05)$ . In [44] Planck-2018 joint constraints on  $n_s$  and  $r$  were used to obtain the constraints on  $\beta$  and it was found that  $1.9 \leq \beta \leq 1.9999$  for  $N_{\text{pivot}} = [50, 60]$ . Our results shown in Table II agree with the analysis of [43,44], however, we have performed a robust statistical analysis by exploring the entire allowable range for the parameters  $\beta$ ,  $M$ , and  $N_{\text{pivot}}$ . With our approach we have obtained the best fit values for these parameters along with their marginalized probability distributions and joint constraints on them, which provides stronger statistical evidence for  $\beta$  lower than 2. The value of  $\beta$  obtained in [45] is slightly

larger than 2 ( $\beta = 2.0008$ ), which deviates by  $2\sigma$  from the best-fit value (27).

It has been shown that the potential for the Starobinsky inflation in the Einstein frame can be obtained from the no-scale supergravity [35–37]. The potential for power law Starobinsky inflation in the Einstein frame from no-scale supergravity is derived by [42]. Since the variants of Starobinsky inflation can be obtained from supergravity, these models play an important role in particle physics phenomenology. The bounds on inflaton potential parameters obtained in this work can be useful to build models of inflation from supergravity that can help us in connecting inflation with other high energy physics phenomena.

## ACKNOWLEDGMENTS

The authors would like to thank Indian Space Research Organization, Department of Space, Government of India to provide financial support via RESPOND programme Grant No. DS\_2B-13012(2)/47/2018-Sec. II.

- 
- [1] A. H. Guth, *Phys. Rev. D* **23**, 347 (1981).
  - [2] V. F. Mukhanov and G. V. Chibisov, *JETP Lett.* **33**, 532 (1981).
  - [3] A. A. Starobinsky, *Phys. Lett.* **117B**, 175 (1982).
  - [4] A. H. Guth and S.-Y. Pi, *Phys. Rev. D* **32**, 1899 (1985).
  - [5] G. F. Smoot, C. L. Bennett, A. Kogut, E. L. Wright, J. Aymon, N. W. Boggess, E. S. Cheng, G. De Amici *et al.*, *Astrophys. J.* **396**, L1 (1992).
  - [6] E. Komatsu *et al.* (WMAP Collaboration), *Astrophys. J. Suppl. Ser.* **192**, 18 (2011).
  - [7] P. A. R. Ade *et al.* (Planck Collaboration), *Astron. Astrophys.* **594**, A20 (2016).
  - [8] Y. Akrami *et al.* (Planck Collaboration), *Astron. Astrophys.* **641**, A10 (2020).
  - [9] J. Martin, C. Ringeval, and V. Vennin, *Phys. Dark Universe* **5–6**, 75 (2014).
  - [10] A. A. Starobinsky, *Phys. Lett.* **91B**, 99 (1980).
  - [11] A. Vilenkin, *Phys. Rev. D* **32**, 2511 (1985).
  - [12] M. B. Mijic, M. S. Morris, and W. M. Suen, *Phys. Rev. D* **34**, 2934 (1986).
  - [13] L. H. Ford, *Phys. Rev. D* **35**, 2955 (1987).
  - [14] H. J. Schmidt, *Classical Quantum Gravity* **6**, 557 (1989).
  - [15] K. i. Maeda, *Phys. Rev. D* **39**, 3159 (1989).
  - [16] V. Muller, H. J. Schmidt, and A. A. Starobinsky, *Classical Quantum Gravity* **7**, 1163 (1990).
  - [17] S. Gottlober, V. Muller, H. J. Schmidt, and A. A. Starobinsky, *Int. J. Mod. Phys. D* **01**, 257 (1992).
  - [18] A. De Felice and S. Tsujikawa, *Living Rev. Relativity* **13**, 3 (2010).
  - [19] S. Nojiri and S. D. Odintsov, *Phys. Rep.* **505**, 59 (2011).
  - [20] S. Nojiri, S. D. Odintsov, and V. K. Oikonomou, *Phys. Rep.* **692**, 1 (2017).
  - [21] A. Codello, J. Joergensen, F. Sannino, and O. Svendsen, *J. High Energy Phys.* **02** (2015) 050.
  - [22] I. Ben-Dayan, S. Jing, M. Torabian, A. Westphal, and L. Zarate, *J. Cosmol. Astropart. Phys.* **09** (2014) 005.
  - [23] M. Rinaldi, G. Cognola, L. Vanzo, and S. Zerbini, *J. Cosmol. Astropart. Phys.* **08** (2014) 015.
  - [24] R. Costa and H. Nastase, *J. High Energy Phys.* **06** (2014) 145.
  - [25] L. Sebastiani, G. Cognola, R. Myrzakulov, S. D. Odintsov, and S. Zerbini, *Phys. Rev. D* **89**, 023518 (2014).
  - [26] Y. F. Cai, J. O. Gong, and S. Pi, *Phys. Lett. B* **738**, 20 (2014).
  - [27] R. Kallosh and A. Linde, *J. Cosmol. Astropart. Phys.* **07** (2013) 002.
  - [28] S. D. Odintsov and V. K. Oikonomou, *Phys. Rev. D* **104**, 124065 (2021).
  - [29] P. A. R. Ade *et al.* (BICEP2 Collaboration), *Phys. Rev. Lett.* **112**, 241101 (2014).
  - [30] J. Martin, C. Ringeval, R. Trotta, and V. Vennin, *Phys. Rev. D* **90**, 063501 (2014).
  - [31] R. Adam *et al.* (Planck Collaboration), *Astron. Astrophys.* **586**, A133 (2016).
  - [32] M. Artymowski and Z. Lalak, *J. Cosmol. Astropart. Phys.* **09** (2014) 036.
  - [33] S. D. Odintsov and V. K. Oikonomou, *Phys. Rev. D* **99**, 064049 (2019).
  - [34] S. D. Odintsov and V. K. Oikonomou, *Europhys. Lett.* **129**, 40001 (2020).
  - [35] J. Ellis, D. V. Nanopoulos, and K. A. Olive, *Phys. Rev. Lett.* **111**, 111301 (2013); **111**, 129902(E) (2013).
  - [36] J. Ellis, D. V. Nanopoulos, and K. A. Olive, *J. Cosmol. Astropart. Phys.* **10** (2013) 009.

- [37] J. Ellis, D. V. Nanopoulos, K. A. Olive, and S. Verner, *J. High Energy Phys.* **03** (2019) 099.
- [38] W. Buchmuller, V. Domcke, and K. Kamada, *Phys. Lett. B* **726**, 467 (2013).
- [39] S. Ferrara, R. Kallosh, A. Linde, and M. Porrati, *Phys. Rev. D* **88**, 085038 (2013).
- [40] F. Farakos, A. Kehagias, and A. Riotto, *Nucl. Phys.* **B876**, 187 (2013).
- [41] S. Ferrara, R. Kallosh, A. Linde, and M. Porrati, *J. Cosmol. Astropart. Phys.* **11** (2013) 046.
- [42] G. K. Chakravarty and S. Mohanty, *Phys. Lett. B* **746**, 242 (2015).
- [43] H. Motohashi, *Phys. Rev. D* **91**, 064016 (2015).
- [44] S. D. Odintsov and V. K. Oikonomou, *Int. J. Mod. Phys. D* **32**, 2250135 (2023).
- [45] S. Meza, D. Altamirano, M. Z. Mughal, and C. Rojas, *Int. J. Mod. Phys. D* **30**, 2150062 (2021).
- [46] S. Santos da Costa, M. Benetti, R. M. P. Neves, F. A. Brito, R. Silva, and J. S. Alcaniz, *Eur. Phys. J. Plus* **136**, 84 (2021).
- [47] M. J. Mortonson, H. V. Peiris, and R. Easther, *Phys. Rev. D* **83**, 043505 (2011).
- [48] A. Lewis, A. Challinor, and A. Lasenby, *Astrophys. J.* **538**, 473 (2000).
- [49] A. Lewis and S. Bridle, *Phys. Rev. D* **66**, 103511 (2002).
- [50] V. F. Mukhanov, *Sov. Phys. JETP* **67**, 1297 (1988).
- [51] M. Sasaki, *Prog. Theor. Phys.* **76**, 1036 (1986).
- [52] B. A. Bassett, S. Tsujikawa, and D. Wands, *Rev. Mod. Phys.* **78**, 537 (2006).
- [53] P. A. R. Ade *et al.* (BICEP and Keck Collaborations), *Phys. Rev. Lett.* **127**, 151301 (2021).
- [54] N. Aghanim *et al.* (Planck Collaboration), *Astron. Astrophys.* **641**, A6 (2020); **652**, C4(E) (2021).